# e.Inspector

## Executive Summary

**Prepared by:**
Michèle Lavagna

**Approved by:**
Michèle Lavagna

**Date of issue:**
28/09/2024

| Change Record | | | |
|---|---|---|---|
| Issue | Date | Change Authority | Reason for Change and affected Section |
| 1.0 | 28/09/2024 | PoliMi | 1st issue. |

## Contents

# 1 Introduction

## 1.1 Scope of the Document

The document synthesizes the results obtained through the performed Phase B for the e.Inspector mission and discussed in deep in the related documentation.

The document is organized as follows:

- first the mission objectives are recalled

- the proposed Mission Analysis and related effects for the baseline target potential changes are presented

- the Service Module design refinement is briefly synthetized, together with the work performed for the IP-GNC base chain with PIL and HIL

- the Ground Segment proposed designed is shortly discussed.

## 1.2 References

### 1.2.1 Applicable documents

In case of conflict between two or more applicable documents, the higher document will prevail. Where no issue or date is specified against a document then the latest version is applicable.

[AD1] ESA-GSTP-TECSPC-SOW-2022-001621 , "Statement of Work - e-Inspector phase B.", ESA, 2021.

[AD2] EINSP- SDR DEL27_v1.0, "System Design Report", Politecnico di Milano, May 2024

[AD3] ECSS-U-AS-10, "Space sustainability. Adoption of Notice of ISO 24113: Space systems – Space debris mitigation requirements." Tech. rep., ESA, 2012.

[AD4] EINSP-DEL-05-MAR, "Mission Analysis Report", Politecnico di Milan

[AD5] EINSP-DEL-01-OBDR, "OBC Breadboard Design Review", Politecnico di Milano

[AD6] EINSP-DEL-24-SCPAR, "Spacecraft Power Analysis report", Politecnico di Milano

[AD7] EINSP-DEL-23, "Propulsion equipment endurance tests report", T4i

[AD8] EINSP-DEL-12 Space-ground interface control document

[AD9] EINSP-DEL-04-GNC Design Definition File

### 1.2.2 Reference documents

The following list of reference document is for general guidance only and need not to be applied, but they should be given precedence over other documents covering similar topics.

[RD1] C. S. R. CDF-174(C), "e.INSPECTOR CDF Study Report," Tech. rep., ESA, 2017.

[RD2] CleanSpace - ESA-TECSYE-TN-010228, "Safe Close Proximity Operations," Tech. rep., ESA, 2018.

[RD3] "VV02 – Vega uses VESPA," http://www.esa.int/Enabling_Support/Space_ Transportation/Launch_vehicles/VV02_Vega_uses_Vespa.

[RD4] "Vega C user manual," https://www.arianespace.com/wp-content/uploads/2018/ 07/Vega-C-user-manual-Issue-0-Revision-0_20180705.pdf.

[RD5] ECSS-E-ST-10-06C, "Space engineering – Technical requirements specification." Tech. rep., European Cooperation for Space Standardization, 2009.

[RD6] "Gecko Imager," https://www.cubesatshop.com/product/scs-gecko-imager/.

[RD7] "FLIR Tau 2 Thermal Camera," https://www.flir.com/products/tau-2/.

## 1.3 Acronyms

| | |
|---|---|
| ACL | Access Control Lists |
| AD | Applicable Document |
| ADR | Active Debris Removal |
| AOS | Acquisition Of Signal |
| API | Application Programming Interface |
| BER | Bit Error Rate |
| CAM | Collision Avoidance Manoeuvre |
| CoM | Centre of Mass |
| CMOS | Complementary metal oxide semiconductor |
| CONOPS | Concept of Operations |
| D/L | Downlink |
| ECI | Earth Centred Inertial |
| EIRP | Effective Isotropic Radiated Power |
| FoV | Field Of View |
| GNC | Guidance Navigation and Control |
| GNSS | Global Navigation Satellite System |
| GS | Ground Segment |
| GSaaS | Ground Segment as a Service |
| GSD | Ground Sampling Distance |
| GSN | Ground Station Network |
| IMU | Inertial Measurement Unit |
| IP | Image Processing |
| ITU | International Telecommunication Union |
| KOZ | Keep Out Zone |
| LEO | Low Earth Orbit |
| LEOP | Launch and Early Orbit Phase |
| LHCP | Left Hand Circular Polarisation |
| LOS | Line Of Sight |
| LVLH | Local Vertical Local Horizonal |
| LVDS | Low voltage differential signalling |
| M2M | Machine-to-Machine |
| MCS | Mission Control Software |
| MGMTR | Magnetometer |
| MOC | Mission Operations Centre |
| MODCOD | Modulation and Coding |
| MTF | Modulation transfer function |
| MTRQ | Magnetorquer |
| NCE | Network Cloud Engine |
| OBC | On Board Computer |
| OBSW | On-board Software |
| OPEX | Operational Expenditure |
| PFD | Power Flux Density |
| QE | Quantum Efficiency |
| REST-API | Representational State Transfer Application Programming Interface |
| RF | Radio Frequency |
| RHCP | Right Hand Circular Polarisation |

| | |
|---|---|
| ROE | Relative Orbital Elements |
| RW | Reaction Wheel |
| RX | Receiver/Reception |
| SS | Sun Sensor |
| SLG | S band Low Gain |
| SHG | S band High Gain |
| SNR | Signal to Noise Ratio |
| SPI | SpaceWire Interface |
| STR | Start Tracker |
| TBC | To Be Confirmed |
| TBD | To Be Determined |
| TCO | Total Cost of Ownership |
| TCP/IP | Transmission Control Protocol/Internet Protocol |
| TIR | Thermal Infrared |
| TLE | Two Line Elements |
| TLS | Transport Layer Security |
| TM | Telemetry |
| TTMTC | Telemetry, Tracking & TeleCommand |
| TT&C | Telemetry, Tracking & Command |
| TRL | Technology Readiness Level |
| TRX | Transceiver |
| TX | Transmitter/Transmission |
| U/L | Uplink |
| VIS | Visible |
| VPN | Virtual Private Network |
| ZTA | Zero-Trust Security Architecture |

# 2 Mission Objectives

The e.Inspector mission aims at a European debris close inspection, possibly in preparation of future ADR missions.
In particular, the main objective of the mission is to inspect a European target and achieving this objective with an imaging payload.
VESPA debris 39162 was the debris identified as the mission target due to the strong interest in imaging it after a recent collision with another debris.
However, at the end of the phase B, due to the stricter regulations imposed on disposal, the baseline moved to the European Proba I spacecraft, still keeping some alternatives the mission design as is can be compliant with.
The mission is performed by a 12U CubeSat, whose design is presented in [AD2], equipped with an electric propulsion for the transfer and disposal phase, and with a chemical thruster to perform the relative maneuvers.
This imposes several system key functionalities, which distinguish this mission.
In particular:

- The spacecraft shall have an adequate authority on its trajectory control to reach the desired absolute orbit of the target, move safely, and according to imaging goals, relatively to the target, and potentially enter a disposal trajectory.
- The spacecraft shall acquire images of the target in proximity, as required for its shape and dynamics reconstruction.
- The spacecraft shall be in contact with ground to download large amount of imaging data and upload re-planning, as needed.

The main mission phases of e.Inspector mission are reported Figure 2-1 together with a simplified timeline. A detailed description of each phase is provided in [AD4].


*Figure 2-1 e.Inspector mission phases*

# 3 Target selection

The target selection of the e.Inspector mission was carried out following three drivers:

- to inspect a European target and achieving this objective with an imaging payload.
- To inspect the VESPA debris.
- To be compliant with the clean space requirement.

In particular it is important to underline that the European regulations in terms of Clean Space are changing, and that drove at the very last phase of the phase B the need to add a second baseline of interest, still European but compliant with the new regulation which imposes to naturally de-orbit within 5 years. VESPA target (~730 km), assumed as primary target all over the phase A/B, doesn't allow a fast natural re-entry, therefore an investigation of possible secondary target that are compliant with the supposed new regulations have been carried out which led to consider Proba I as the new baseline for the next phases. Still the other alternatives are kept to perform the mission design refinement.

## 3.1 VESPA debris

VESPA-39162 debris, was proposed by the Agency in the phase A SoW and was considered as baseline in the Phase A study. VESPA is an adapter of the VEGA launcher injected in orbit in 2013 during the launch of the Proba-V spacecraft, as shown in Figure 3.1-1.


*Figure 3.1-1: VESPA with Proba-V on its top. credits:*

The VESPA orbit was propagated using a in-house-developed high-fidelity propagator starting from the TLEs available on the NORAD catalogue and reported in Table 3.1-1 . It is important to underline that the orbit of VESPA is not exactly a Sun Synchronous Orbit (SSO), and therefore the Local Time of its Ascending Node is not constant in time, showing an average precession of 1.2 h/y.

This aspect implies that a change in the launch epoch has a strong influence both on the platform design and on the launch selection. Indeed, on one hand the illumination conditions of the target and of the service module are different at different LTAN, and consequently on the launch epoch; on the other hand, a change in the launch epoch would change the relative distance between the launcher injection and the target actual plane, leading to a change in the transfer cost and time that could exceed the capabilities of the platform. For those reasons, the transfer phase analysis is conducted with a parametric approach with respect to the altitude of the launch and the difference between the injection and target LTANs.

*Table 3.1-1: VESPA orbital elements.*

| Parameter | Value |
|---|---|
| **Semi-major axis [km]** | 7097.09966 |
| **Eccentricity [-]** | 0.0091895 |
| **Inclination [deg]** | 98.7254 |
| **RAAN [deg]** | 87.7009 |
| **Arg. Of perigee [deg]** | 113.4314 |
| **Mean anomaly [deg]** | 247.6574 |
| **Epoch [dd/mm/yyy]** | 08/06/2024 |

## 3.2 Low-altitude backup targets

In order to be compliant with future regulations concerning space cleanness, secondary targets below a selected altitude threshold have been select. The threshold of altitude has been identified after a Montecarlo decay analysis.

In particular, the orbital lifetime was estimated, as shown in Figure 3-4, as function of the ballistic coefficient and the initial altitude. On the same plot, the estimated ballistic coefficient of the CubeSat with both folded and deployed solar panels is reported. The safe altitude (95% of confidence) is ~460 with folded solar panels, as during the LEOP, and ~490 km with deployed solar panels, namely during the transfer and inspection phases. The confidence levels reported in Figure 3.2-1 represent the fraction of runs that decay given a certain altitude and ballistic coefficient. Table 3-2 lists the parameters included as uncertainties in the Montecarlo simulation.

*Table 3.2-1; Uncertainties included in MC simulation.*

| Parameter | Uncertainty (Type) | Uncertainty (Value) |
|---|---|---|
| **Semi-major axis** | Uniform | 6778 km – 6978 km |
| **Eccentricity** | Normal (bounded) | Mean: 0<br>Dev Std: 0.00008<br>Boundaries: 0 – 0.0001 |
| **Inclination** | Uniform | 97° - 99° |
| **Epoch (initial)** | Uniform | 2026 – 2035 |
| **Mass** | Uniform | 18 kg – 26 kg |
| **CD** | Normal (bounded) | Mean: 1.9<br>Dev Std: 0.2<br>Boundaries: 1.5 – 2.2 |
| **Cross section (drag & SRP separately)** | Normal (bounded) | Mean: 0.25 $m^2$<br>Dev Std: 0.1<br>Boundaries: 0.04 $m^2$ – 0.445 $m^2$ |
| **Reflectivity** | Uniform | 0.5 - 2 |

The problem of selecting a secondary target below the safe altitude has been addressed at the end of the phase B, however it is important to underline that the high drag environment induces also a relatively fast decay of the debris that are in such belt, therefore the stability of the target orbit over long period is not ensured, and a delay in the project could lead to the necessity to switch to other targets.

Through CelesTrack the cumulative distribution of debris below a certain altitude has been identified, no matter of the nationality and the kind of debris (i.e. Rocket bodies and general debris).

Table 3.2-2 and Table 3.2-3 show the pruning process of the on-orbit debris: at this time there are only 3 European debris below 500 km of altitude (marked with IDs), and only 1 of them shows an RCS larger than 1 m2.

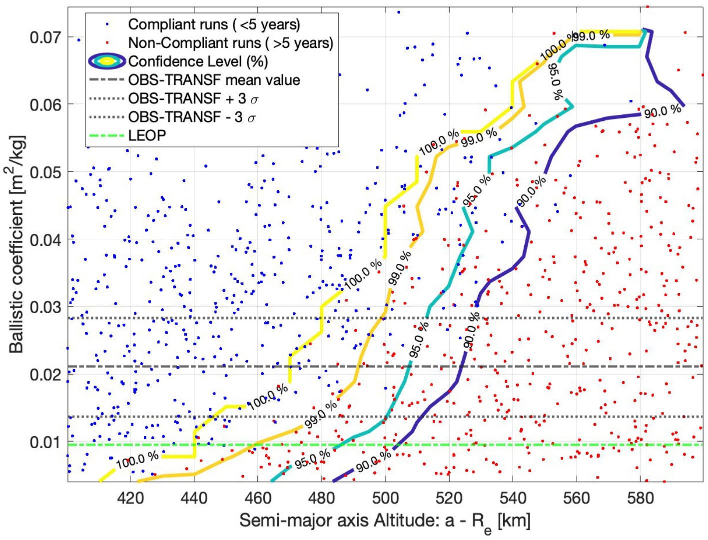


*Figure 3.2-1 Orbital lifetime – 5 years natural decay.*

*Table 3.2-2: Debris pruning – all bodies.*

| **Natural reentry time** | **25 years** (h<575km) | **5 years** (h<500km) |
|---|---|---|
| All debris | 777 | 394 |
| **All debris (European)** | **11** | **3** |
| Rocket bodies | 146 | 71 |
| **Rocket bodies (European)** | **4** | **0** |

*Table 3.2-3; Debris pruning – high RCS bodies.*

| **Natural reentry time** | **25 years** (h<575km) | **5 years** (h<500km) |
|---|---|---|
| All debris | 67 | 22 |
| **All debris (European)** | **5** | **1** |
| Rocket bodies | 54 | 16 |
| **Rocket bodies (European)** | **3** | **0** |

Due to the low number of targets below 500 km, and due to their limited orbital lifetime, in accordance with the Agency, backup targets are chosen below 575 km. The most promising targets are listed in the followings. NORAD object 26958, PROBA-1 spacecraft, is added to the list as it is the new target of the ClearSpace mission and is located at a relatively low mean altitude of 564 km.

### 3.2.1 Target 23608

The first backup target identified is NORAD catalogue object 23608, whose extended name is ARIANE 40+3 R/B, a rocket body larger than VESPA with an average altitude of ~532 km, as can be seen from the orbital elements extrapolated form TLEs and listed in Table 3.2.1-1.

This target, like VESPA, is not exactly located in Sun-Synchronous Orbit, but shows an average LTAN variation of about +2.1 h/y. In addition, it is possible to observe by looking at the altitude evolution that the rocket body shows progressive orbital decay caused by atmospheric drag.

*Table 3.2.1-1: 23608 orbital elements.*

| Parameter | Value |
|---|---|
| **Semi-major axis [km]** | 6911.050765 |
| **Eccentricity [-]** | 0.0016971 |
| **Inclination [deg]** | 98.2514 |
| **RAAN [deg]** | 281.5357 |
| **Arg. Of perigee [deg]** | 94.1727 |
| **Mean anomaly [deg]** | 266.1440 |
| **Epoch [dd/mm/yyy]** | 08/06/2024 |

### 3.2.2 Target 25979

The second backup target identified is 25797, whose extended name is ARIANE R/B, a rocket body with an altitude of ~550 km, as can be seen from the orbital parameters extrapolated from TLEs and reported in Table 3.2.2-1. Also this target is not exactly located in an SSO, with an average LTAN variation of +2.1 h/y. Again, it is possible to observe the progressive orbital decay of the rocket body subjected to atmospheric drag.

*Table 3.2.2-1 25979 orbital parameters.*

| Parameter | Value |
|---|---|
| **Semi-major axis [km]** | 6917.983228 |
| **Eccentricity [-]** | 0.0008462 |
| **Inclination [deg]** | 98.2418 |
| **RAAN [deg]** | 174.2940 |
| **Arg. Of perigee [deg]** | 114.1906 |
| **Mean anomaly [deg]** | 246.0206 |
| **Epoch [dd/mm/yyy]** | 08/06/2024 |

### 3.2.3 PROBA-1 (26958)

As previously anticipated, the last backup target identified and assumed as baseline for the next phases is PROBA-1 (NORAD object 26958), a spacecraft with a mean altitude of 564 km, as can be seen from the orbital parameters in Table 3.2.3-1 and from the orbital propagation reported in Figure 3.2.3-1. The plots display that this target is not exactly located in an SSO, showing an average LTAN variation of +0.65 h/y.

Finally, a slightly slower orbital decay due to atmospheric drag is observed with respect to the two previous low-altitude targets.

*Table 3.2.3-1: PROBA-1 orbital parameters.*

| Parameter | Value |
|---|---|
| **Semi-major axis [km]** | 6941.779573 |
| **Eccentricity [-]** | 0.006002 |
| **Inclination [deg]** | 97.9160 |
| **RAAN [deg]** | 135.4300 |
| **Arg. Of perigee [deg]** | 95.9270 |
| **Mean anomaly [deg]** | 264.8780 |
| **Epoch [dd/mm/yyy]** | 08/06/2024 |

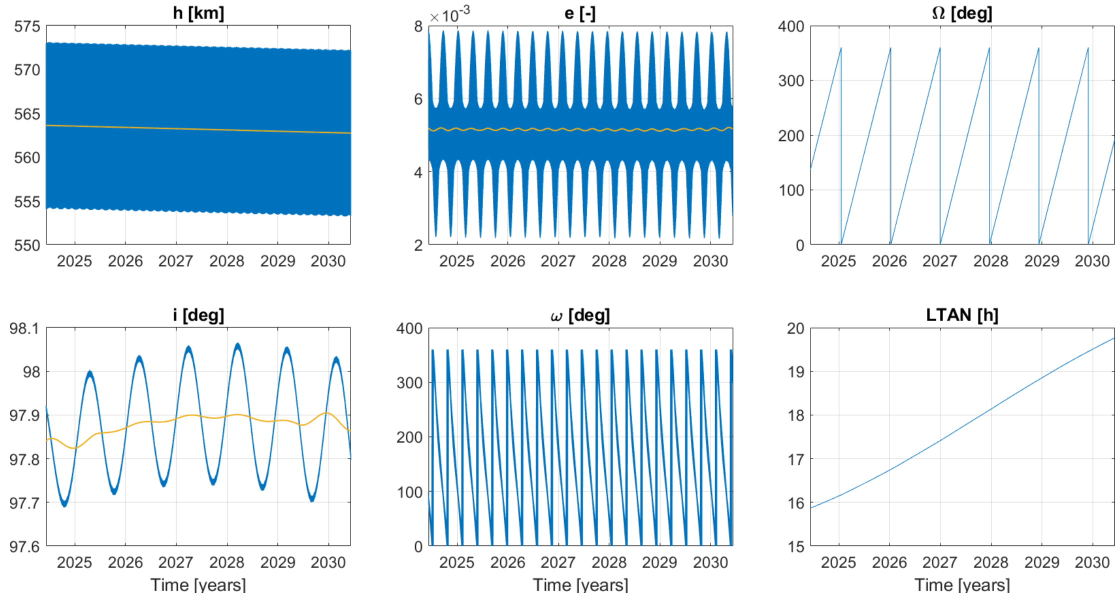


*Figure 3.2.3-1: PROBA-1 orbit propagation.*

# 4 Mission concept

Figure 2-1 synthetically shows the e.Inspector mission phases the most sizing being the transfer and the inspect, being the strong constraint imposed by the disposal regulation already discussed.

## 4.1 Transfer phase

Since e.Inspector will be launched as piggyback of a main payload it is expected to be released in a different SSO orbit with respect to the target's. Therefore, the plane change is the most demanding manoeuvre which is solved by exploiting the J2 drift combined with low thrust trajectory control, paying the price of a long transfer to target, between 6 and 12 months, with a strategy schematized by Figure 4.1-1 [AD2].

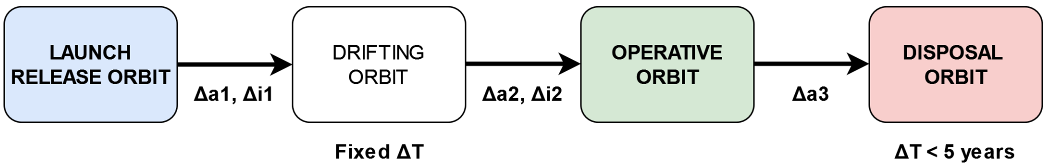


*Figure 4.1-1: baseline transfer phases.*

Figure 4.1-2 shows the maps of the assessment of feasibility with respect to the new 5 years disposal regulation adopting the performance of the thruster selected as baseline along the phase B(Regulus 50, t4i). The feasibility is reported in terms of attainable LTAN variation, launcher release orbit altitude and orbital plane drift duration. To consider non nominal conditions, at the launcher release as well, a maximum altitude of 430 km has been identified to ensure a reentry in 5 years If any anomaly happens at the launcher release. The maps also include the boundaries ( green line) of the ΔV that can be reached with the baseline (Regulus 50, t4i) minus the ΔV that is need for disposal according to the specific target debris. showing the maximum launch admissible ΔLTAN and Δa boundaries. The maps highlight that VESPA is not manageable with the new regulations; the other three potential targets can be reached while being compliance with the disposal regulations even in case of non nominality occurring at the release epoch.

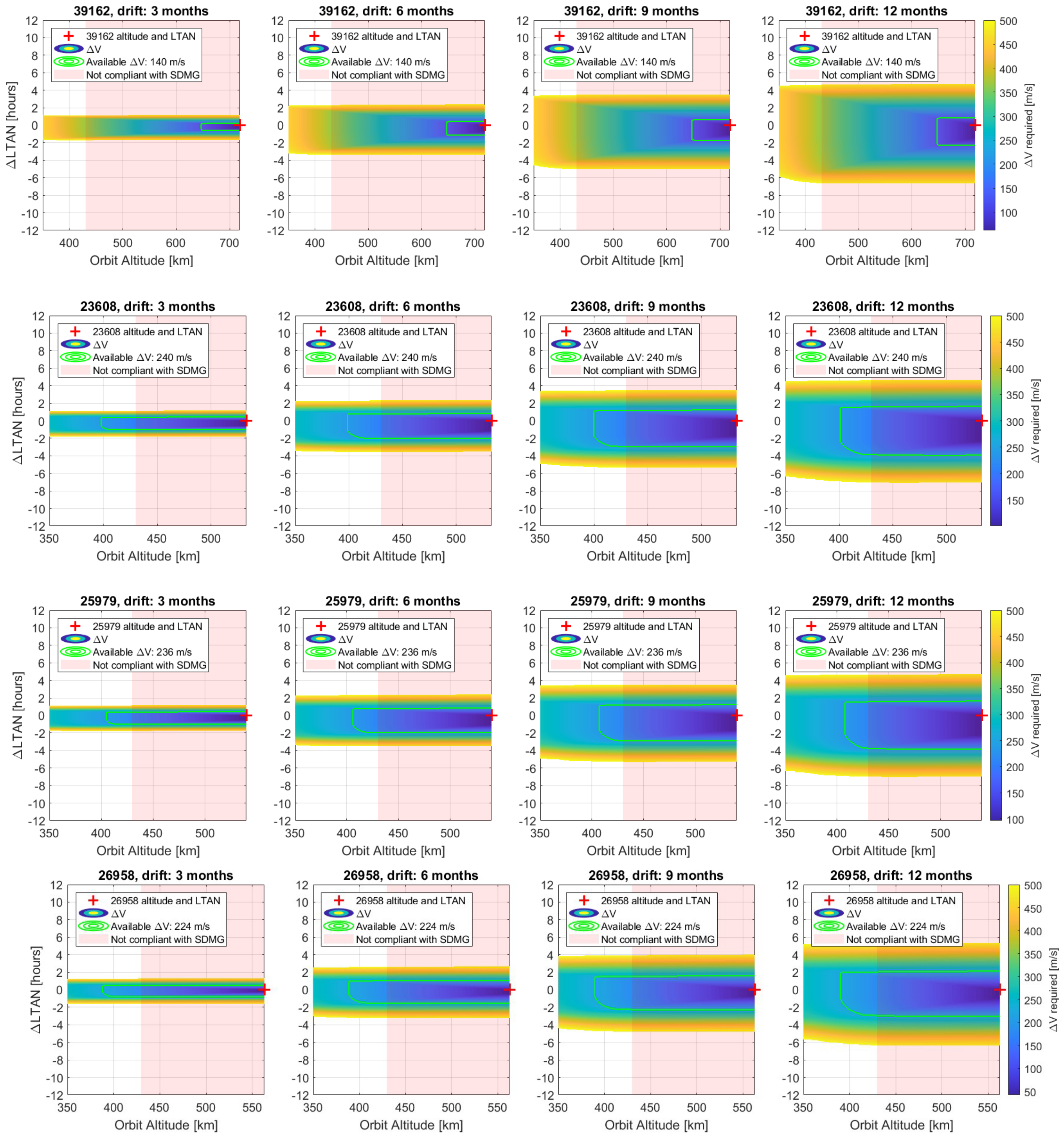


*Figure 4.1-2: ΔV maps for Launch-to-Operative orbital transfer as a function of starting altitude and ΔLTAN, indicating feasible launch region taking space debris mitigation into consideration. Rows refer to possible target debris considered.*

### 4.1.1 Launchers selection

It is important to underline that the identification of the exact launch is not possible in this phase since the LTAN of the targets changes with the epoch, and therefore a change in the launch date will change also the cost of the transfer, with a potential impact on the transfer feasibility.

Since launches in SSO are extremely frequent, in accordance with the Agency the problem has been reverted and translated into the analysis of requirements for the launch selection in terms of ΔLTAN and injection altitude as presented in the previous transfer analysis.

Table 4.1.1-1 shows a partial list of European launches planned for the window of interest of the e.Inspector mission. Unfortunately, no scheduled European launch that will fly in the following years is able to reach directly the region of interest close to the targets. To drive the future selection of a possible candidate launch, two requirements have been added on the maximum LTAN and altitude distance with respect to the target orbit (see req. M-0414/415).

*Table 4.1.1-1: Launch opportunities.*

| EUROPEAN OPTIONS | | | | |
|---|---|---|---|---|
| **Mission** | Expected date | Altitude [km] | LTAN [hh:mm] | Launcher |
| **Sentinel CO2M-A** | 2026 Q1 | 735 | 23:30 | Vega-C |
| **METOP-SG B1** | 2026 Q4 | 835 | 21:30 | Ariane-62 |
| **Sentinel CO2M-B** | 2026 Q2 | 735 | 23:30 | Vega-C |
| **SSMS #14** | 2026 Q2 | 680 | 22:00 | Vega-C |
| **CSG-4** | 2026 Q2 | 620 | 6:00 / 18:00 | Vega-C |
| **MERLIN** | 2027 | 500 | 6:00 / 18:00 | Vega-C |
| **Sentinel CO2M-C** | 2027 Q3/Q4 | 735 | 11:30 / 23:30 | Vega-C |
| **FORUM** | 2027 Q3 | 830 | 9:30 / 21:30 | Vega-C |
| **Sentinel-3D** | 2028 | 810 | 22:00 | Vega-C |
| **LSTM** | 2029 Q1 | 651 | 00:30 | Vega-C |
| **CIMR-A** | 2029 Q3 | 830 | 18:00 | Vega-C |
| **CHIME** | 2029 Q4 | 632 | 22:45 | Vega-C |
| **SSMS #21** | 2029 Q4 | [TBD] | [TBD] | Vega-C |
| **Harmony 1/2** | 2029 Q4 | 693 | 18:00 | [TBD] |

In addition to these European options, other scheduled rideshare missions by SpaceX are already scheduled for 2026 (Q1, Q2, Q4) and 2027 (Q1, Q2, Q4).

## 4.2 Image target phase

Within the mission operational phase, the imaging functionality is twofold, as it allows collecting data useful for a future ADR mission and, as a byproduct, exploiting the imaging sensors to perform visual based navigation. Therefore, while the focus stays in the target inspection, benefits for on orbit navigation are considered as well. The imaging architecture was selected considering quite stringent requirements and different criteria here reported:

- Inspection Data. Quality, quantity and type of collected information shall be maximized, considering the materials that are observable among MLI, solar cells, aluminium, CFRP.
- Operational Flexibility. The easier the imaging system exploitation during operations the more robust and powerful the mission turns to be.
- Complexity. The imaging system shall have a low complexity, allowing an easy on-board management of payload data.Mass. The imaging system mass shall be low.

- Navigation Robustness. The imaging system should possibly benefit the navigation robustness, giving the possibility to exploit measurements from such sensors for the navigation.

Among the requirements strictly connected to the inspect phase design, just the most demanding are here reported to better perceive the challenge of the e.Inspector mission design:

- the image resolution when imaging the capture interfaces of the target shall be lower than 1 cm.
- the OBDH shall autonomously process images.
- the GNC system shall estimate position and velocity of the spacecraft in a target centred reference frame (relative position and velocity).
- the GNC system shall estimate the attitude of the spacecraft with respect to the target-fixed reference frame (relative attitude) with a maximum error of 3° with 95% probability.

To answer the mission needs, between the two alternatives VIS only and VIS+IR, the latter has been confirmed in phase B as baseline for imaging measurements along the mission. T
he choice offers a broader domain of observable materials for longer, being the IR sensor exploitable even on the shadowed target (i.e. eclipses).
Moreover, two sensors on board represent a hot redundancy scheme for the mission robustness.
Taking into account, the operational range, the resolution and the data volume to process, a monocular camera scheme has been preferred against the stereo architecture: one for all, a CubeSat offers no adequate baseline size to go for the latter.
The needed resolution of 1 cm is obtained, and the mass and volume can be kept contained, suitable for a CubeSat hosting.
A large FoV (around 12 deg) helps for target pointing, while the larger computational cost turns into a requirement for a light on-board image processing algorithm to be selected.
The IR band interesting for this mission scenario is therefore the LWIR, since in this band the reflected radiation component is less than the thermal emitted component, allowing robustness to illumination and target visibility also in eclipse (lowest temperatures). The choice of such band can be considered robust with respect to orbit and target materials, since the appropriate band would be always the LWIR.
Concerning the VIS camera, an RGB sensor is preferred, in order to enrich the inspection data with colour information of the target materials. An IR sensor lower resolution is acceptable, as typical for such instruments.

### 4.2.1 Proximity Operations

The image target phase is the most critical part and the ultimate objective of the mission.
The relative trajectories must be passively safe, hence natural motion shall be explored in order to achieve relative orbits, which do not threaten the safety of the image target phase. The imposed criteria to run the selection of the imaging relative trajectories were the passive safety, the variance of geometric coverage and the Sun phase angle & FoV acquisition.
A set of drifting passively safe trajectory is considered as baseline for the relative dynamics. Even if passive safety is ensured, Collision Avoidance Manoeuvre capability is taken into account if navigation estimation covariance enlarges or ground segment telecommands it. Refer to [AD9] for the design description of such trajectories.
The images acquisition windows during the inspection phase have been designed considering the eclipses, the phase angle, the Earth presence in the scene avoidance, the resolution maximization but also the on-board memory capacity and downlink windows frequencies. The proximity operations are split in the following phases:

- Hold points: fixed along-track separation in stable condition. The HP serves as standby safe location. The HP represents the transition between the absolute orbital transfer and the initiation of the inspection operations. HP is used to acquire the target, perform the relative GNC commissioning and initiate the proximity operations.
- Hold orbits: The Hold Orbits are out-of-plane orbits centred along-track at a desired instance from the target. Hold Orbits are used after every inspection trajectory. Hold orbits are used to establish ground contact and perform necessary downlink of imaging data, as well as performing commissioning and check before lowering the distance from the target.
- Relative Orbit transfer manoeuvres: thrusted transfer between relative orbits for phase transition, i.e. approaching the target in a closer/larger configuration.
- Inspection trajectories: ballistic orbits initiated right after manoeuvres, exploited to image the target. Nominally, the inspection phase lasts two month.

Nominally, the inspection phase lasts two months: 30 days are dedicated to the target acquisition along-track, the relative GNC commissioning and the proximity manoeuvre initiation. The duration of the inspection phase may be resized to meet the nominal mission duration based on the selected launch. It is also foreseen that in case of non-nominal scenario Collision Avoidance Manoeuvres (CAMs) are triggered to avoid collision with the target. During such manoeuvres, no dedicated holding-point is targeted, but as soon as the GNC logic detects a distance to the target below a certain threshold, a back-firing action is triggered, until a safe distance is reached. After that, the nominal orbit is recovered by the implemented guidance scheme. Figure 4.2.1-1 and FIgure 4.2.1.2 show the proximity phase orbits and the breakdown of each relevant step timeline respectively.

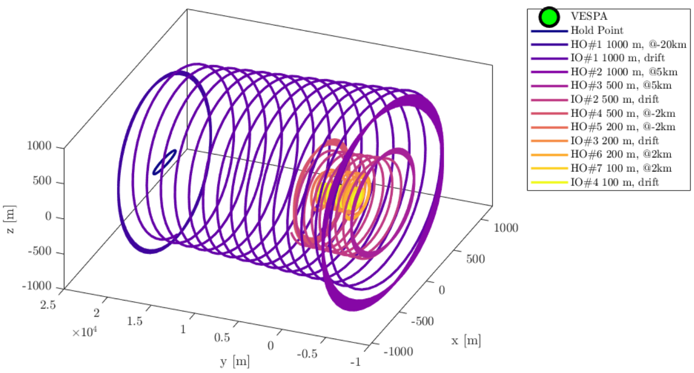


*4.2.1-1: inspection trajectories in the LVLH frame.*

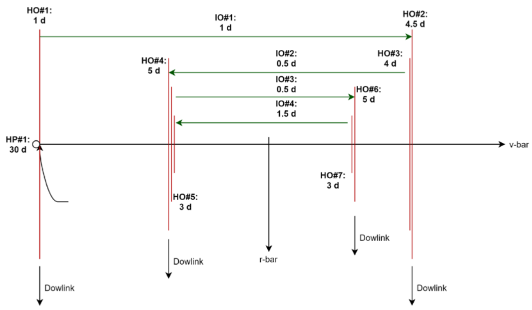


*Figure 4.2.1-2: geometry of the inspection and hold orbits.*

In case of any critical anomaly, a safe mode is triggered to the spacecraft. Such safe mode is power/attitude stable, intended for prolonged periods waiting for operators troubleshooting and command issuing. During the inspection phase, the safety is ensured by passively-safe trajectories and by prompt CAM functionalities.

# 5 Space segment design

## 5.1 Payload design

The baseline, already proposed in phase A, has been defined considering the following driving requirements:

- Available volume in the CubeSat structure
- Mass constraints
- Operative spectral range
- Compatibility with the space environment
- Budget hypothesis

The current payload baseline hypothesis consists in two different cameras:

- Visible camera: GECKO Imager
- TIR camera: FLIR TAU 2

Gecko imager by Dragonfly Aerospace (South Africa) has already flight heritage, therefore there will be no need of qualification activities or verification in terms of space environment compatibility.The camera offers an array of 2048 x 2048 pixels and a FOV of about 9.15 degrees, which satisfies the 1cm/px requirement @100m.

The second payload is the FLIR TAU2 camera, already operative in space. It has an array of 640 x 512 pixels and a FOV of about 6.2 x 5 degrees, slightly over the 1cm/px at 100m.

The target variation toward Proba I it is not expected to be an issue, just a minimum distance proper scaling.

Along phase B EMs for both cameras have been acquired; both of them have been exploited to breadboard the PIL and HIL activities on the IP chain [RD9].

Test campaign to verify the TIR survivability to the space environment is foreseen on the next phase, also considering a possible ruggedization of the hardware [RD2].

Figure 5.1-1 shows that imagers ensure a minimum size of about 7 (TIR) and 15 (VIS) pixels at 2km of distance, where short exposure images are used verifying that the target size is not in the subpixel region. The discussion is referred to the 2 km threshold, since the close-range IP is foreseen to start at that relative distance. For the range 2-20 km, long-exposure images with line detection is used. The switch between the two modes is dependent of target size in image. By looking at the percentage of coverage of the target in the image, it can be noticed that in the closest approach it is about 20% (VIS) and 60% (TIR), confirming that also in the closest approach the target is not cropped and can be completely visible inside the FOV. The characteristic size of VESPA is considered to be 2.4 m [RD9].

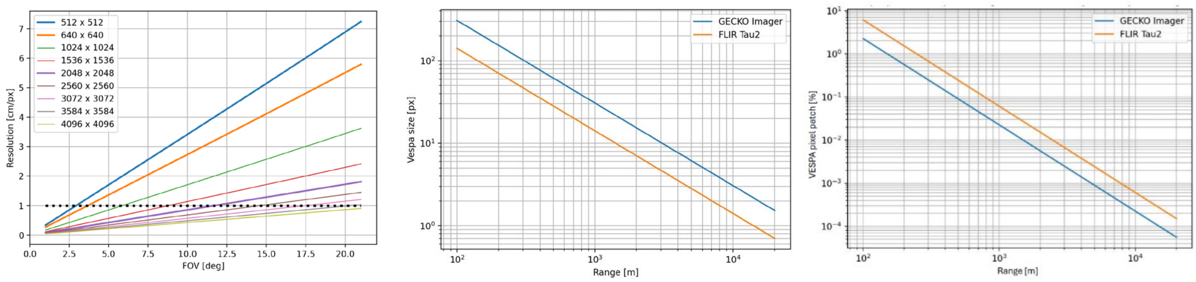


*Figure 5.1-1: Resolution as function of array size; Vespa size in pixel wrt distance. Coverage % of the FOV wrt distance*

## 5.2 Service module design

### 5.2.1 Navigation Guidance and Control (GNC) design

In phase B the IP based navigation was largely dealt with to assess the on board computational

architecture needed and to develop the correspondent software. Therefore activities were articulated in VM, PIL, HIL developing and testing. Figure 5.2-1 a) shows the test plan adopted along the phase B. The virtual framework asked for developing VIS IR synthetic images generators, IP blocks, dynamics simulators, LOS and pose extraction and filtering blocks and it is schematically represented in Figure 5.2-1 b). The VIS image sensor and the OBC-CAM models were then substituted with HW to run the PIL and HIL respectively.
Figure 5.2-2 shows some pictures of the HIL: the VIS camera installed on the robotic arm to acquire sequence of proximity real images of the VESPA mockup in the far and close range scenarios; outputs are shown in the two presented pictures in b).

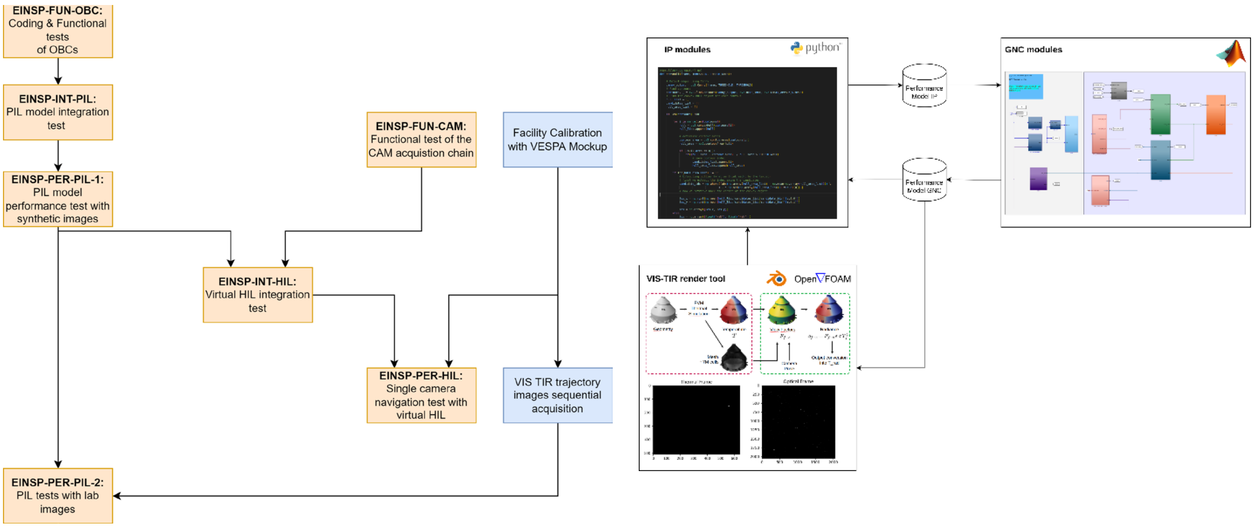


*Figure 5.2-1 a) Test plan flow* *b) virtual model blocks*

*Figure 5.2-2 a)GECKO on arm for real images acquisition b) close\far VESPA imaging – real outputs in lab*

Relative navigation is composed by image processing (IP) algorithms and estimation filtering techniques [RD9]. Please note that relative navigation is a mission driver, being a critical mission operation essential for satisfying the inspection phase and posing several challenges to the bus and payload design, related to computational power requirements and target observing conditions (distance, illumination). The main task for the relative navigation subsystem is the estimate of the relative state (position and velocity) performed on board.
The VIS and IR sensors with their relevant performance presented in the payload section are assumed to be the only source of measurements available for the relative navigation.
Depending on the object size in pixels, the identified approaches are reported in Table 5.2-1.

*Table 5.2-1 IP adopted techniques.*

| Distance | Navigation task | IP Technique |
|---|---|---|
| 20 000 to 900 m | Estimate relative position and velocity | Long exposure images |
| 20 000 to 900 m | Estimate relative position and velocity | Short exposure images - Disparity |
| 900 to 100 m | Estimate relative position and velocity | Centroid - VIS |
| 900 to 100 m | Estimate relative position and velocity | Centroid - IR |
| 200 to 100 m | Estimate relative attitude | Features detection and matching |
| 200 to 100 m | Estimate relative attitude | Model matching |

- **Centroid - IR**. It is possible to exploit this technique with both IR and VIS. IR images are robust to illumination conditions when the phase angle Sun-target-chaser is high.
- **Features detection and matching**. A features map is built by optical features extraction and tracking between subsequent frames. The pose is recovered by comparison with a target features map generated on ground. It provides the relative pose measurement.
- **Model matching**. If prior information on the debris are exploited, a model matching can be performed. The target is detected in the image. Edges are detected and the corresponding model is fitted with a pre-stored shape model of the target. It provides the relative pose measurement.

When the target is farther than 200m, the LoS is the only measurement type that can be derived from the IP. Exploiting information on the object size in the image would not provide accurate range measurement, because the apparent object size in the image is largely affected by illumination conditions.
The IP technique shall be selected depending on the portion of the image occupied by the object and on the navigation task. For what concerns relative pose estimation in the VESPA case, the trade-off i between model matching and feature-based algorithms led to the model matching preference. In fact, the target has likely a known shape, therefore this information is already available for model matching. Moreover, even in close proximity IO, VESPA dimension is still quite small (100-200 pixels), resulting challenging for a vision-based relative pose estimation. In particular, for a feature-based algorithm a low number of features can be extracted, so the algorithm robustness is low.
VESPA has a conic shape, therefore a rotation on the symmetry axis cannot be easily observed. The target spin axis orientation is unknown and in case this issue arises, the error on the estimated relative pose will be large.
For what concerns the state estimation, the IP provides only a LoS measurement. Since the target/chaser distance is extremely variable during Inspection Orbits, at least two different navigation modes are needed:

- when the target size is larger than 10 pixels, the centroid algorithm can be used. Such algorithm is simple to implement and computationally cheap. The best solution exploits both VIS and IR images: visible images grant a better accuracy, but the correct illumination conditions are hard to be met; IR images grant robustness to illumination provide and measurements also during eclipses. Both VIS and IR centroid are proposed, since this is the most robust and accurate solution, with an acceptable computational cost.
- When the target size is smaller than 10 pixels, a simple centroid algorithm cannot be used, because the target identification is not trivial. To use short exposure images is not robust because of the variable phase angle (20° to almost 180°). For this reason, long exposure images strategy is proposed as baseline. Please note that the exposure time is to be assessed during the camera in-flight calibration. Example of long exposure IP is given in Figure 5.2-3 with inertial pointing, adopted whenever a low illumination conditions apply.

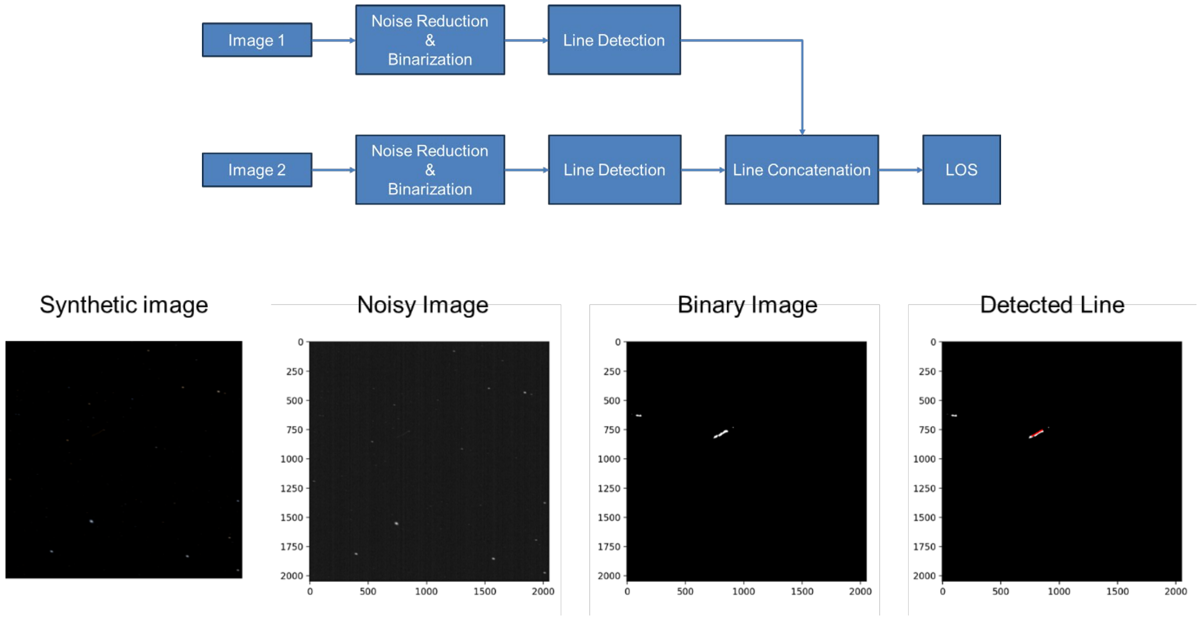


*Figure 5.2-3 Far range-long exposure, inertial pointing: workflow and outputs*

IP is then followed by filtering which has been selected to adopt a differential absolute filtering approach. In fact, the LOS output by the IP makes the problem not fully observable and asks for maneuvering to vary the LOS and gain the observability along the rendez-vous phase. Details are given in [AD9].

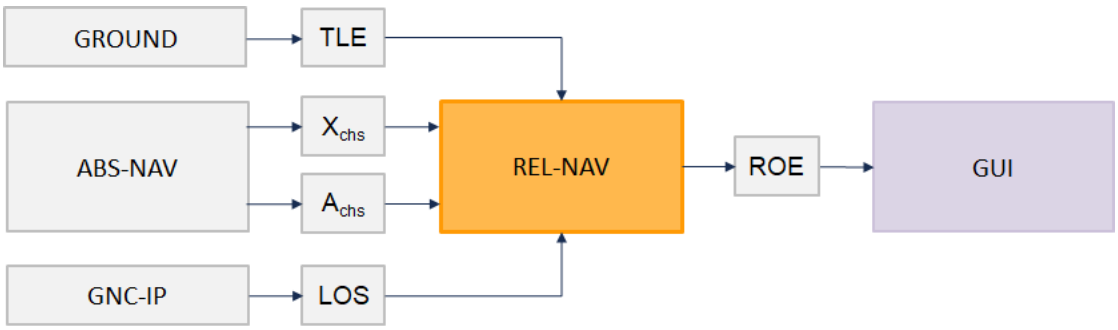


The absolute navigation baseline uses GNSS sensor for absolute position, relative navigation cameras for relative position, and relative attitude estimation in the extended operations, and star tracker for absolute attitude. Star trackers and GNSS sensors are selected because their accuracy is better than the required determination accuracies.
The spacecraft is mounting a star tracker to provide accurate attitude determination. The selection of the component is the output of a comprehensive trade-off analysis [AD2], [AD).
The most important criterion is the max slew rate, which if too low makes the attitude determination impossible, and the component size. The preferable choices coming out from the analysis is the Sagitta Star Tracker by Arcsec.
The GNSS sensor is the Novatel OEM719, with COCOM limit removed, which can guarantee an absolute position accuracy of 1.5m, and a velocity accuracy of 0.03 m/s.
The 6DOF IMU is used in the navigation algorithms to filter the raw data coming from the sensors. Moreover, it is used to propagate dynamics whenever measured data are not available. An excellent IMU

is selected within the CubeSat market. In particular, the IMU in the baseline is the MS-IMU3050M by Memsense Inc. The IMU has 2.6μg and 0.3 $°h^{-1}$ of accelerometer and gyroscope bias instability. The random walk is limited to 0.006 $m/s/h^{-1/2}$ and 0.066 $°/h^{-1/2}$. These values guarantee a propagation error lower than 0.1° and 1m for 20 min of dynamical propagation. These performances are contained in a small component with a mass of 90 g and a power consumption of 2.5 W. Its full specifications are reported in Table 3-9. Two hard redundant IMUs are placed on-board, especially to reduce the risk of losing acceleration measurements without which the navigation filter could not estimate the thruster action.
Redundant secondary navigation sensors are included. Sun sensors and magnetometers are selected to have a complete attitude reconstruction in case of a failure in the star tracker, with reduced performances (AKE 0.5°). Moreover, the magnetometer is used for magnetic actuation during detumbling and desaturation manoeuvres.
The Sun sensors are the GOM space FSS, which are based on quadrant photo-diode technology. They are selected thanks to their wide FOV 120° and the high accuracy ≤0.5°. They will be installed to have complete sky coverage for fast attitude reconstruction. 2 Sun sensors, due to hard redundancy, are installed along any of the 6 body directions, for a total of 12 Sun sensors. Their limited mass ≤3g and the low power consumption ≤15mW make possible the hard redundancy within the CubeSat configuration limits.
The magnetometer is the PNI RM3100, which was selected because of its high accuracy, 15nT and low weight 8g.
All components are TRL 9 with extensive proven flight heritage. They are summarized in Table 5.2-2.

*Table 5.2-2: Attitude determination on-board sensors.*

| **Sensors** | **Model** | **Critical performance** | **TRL** | **Number** |
|---|---|---|---|---|
| Star Tracker | Sagitta ST – Arcsec | Accuracy = 2arcsec | 9 | 1 |
| IMU | MS-IMU3050M – Memsense Inc. | Instability = 2 μg,0.3°$h^{-1}$ | 9 | 2 |
| GNSS sensor | OEM719 – Novatel Inc. | Accuracy = 15m, 0.03m/s | 9 | 2 |
| Sun sensor | FSS – GOM Space | FOV = 120° | 9 | 12 |
| Magnetometer | RM3100 – PNI Sensor Corp. | Accuracy = 15nT | 9 | 1 |

Attitude control actuators are a set of 4 redundant reaction wheels in pyramidal configuration, coupled with 3 orthogonal magnetic torquers. Actuators selection is performed sizing the sub-system on the worst-case manoeuvres. In particular, the slews during the inspection in target pointing and inspection phase shall be feasible without wheels saturation.
The reaction wheels choice is based on a detailed trade-off analysis driven by the flight heritage and the actuators' performances needed to fulfil the requirements underlined before. In Table 5.2-3 the reaction wheels finally selected are listed together with their most important characteristics.

*Table 5.2-3: Reaction wheels trade-off analysis.*

| | Producer | Wheel Momentum Storage | Maximum Torque | TRL |
|---|---|---|---|---|
| RW400 | Hyperion Technologies | 50 mNms | 8 mNm | 9 |

RW400 by Hyperion Technologies B.V. can store 50mNms each, which is a large value in the EU CubeSat market. The 4 reaction wheels assembly in pyramidal configuration can store the worst-case momentum,

even if it is accumulated on a single axis. The maximum torque provided by each single wheel (e.g. 8mNm) is sufficient to guarantee a great excess of control authority in the worst-case scenario with thruster misalignment (e.g. assumed a thruster misalignment equal to the maximum physical dimension in the CubeSat configuration).
The baseline magnetorquers are the GST-600 by GOM Space, including 3 orthogonal magnetic torquers to detumble the spacecraft after the orbital injection and to desaturate the reaction wheels. Moreover, they can be used as redundant secondary actuators in case of wheels failure. In the latter case, only lower pointing performances will be available (e.g. reduced APE). However, this is a true failure case, which would happen after a complete failure of all the 4 reaction wheels.
The minimum dipole moment is sized assuming to detumble the spacecraft in 5h and to achieve 70% desaturation of a single wheel in 3 h.
The baseline GNC architecture features several HW and SW components. A detailed schematic of the architecture is provided in general in Figure 5.2-4.

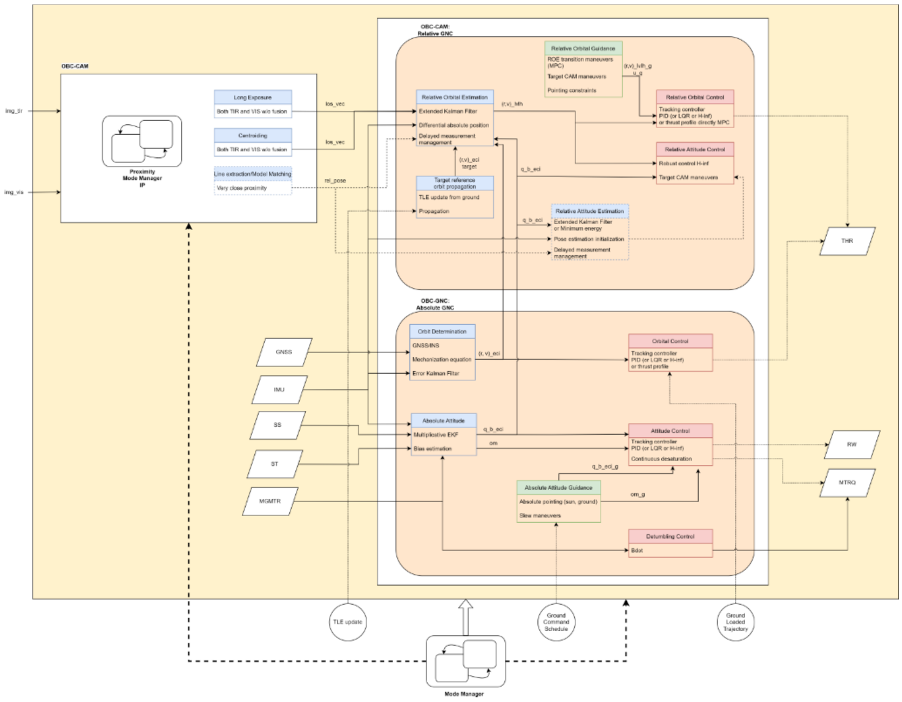

*Figure 5.2-4: Full GNC schematics*

## 5.2.2 Propulsion sub-system design

The spacecraft is equipped with two different propulsive units:

- A **Primary Propulsive Unit** for the transfer phase and for the drag compensation (if needed, depending on the target and injection orbits altitude). Due to the high total impulse required during the transfer phase, an electric unit is needed.
- A **Secondary Propulsive Unit** for the manoeuvres performed in the relative environment and during the inspection. Due to the high controllability needed during the relative manoeuvres, a chemical unit is embarked.

The complete $\Delta V$ budget is in [AD4].

### 5.2.2-1 Primary Propulsive Unit

The primary propulsion is the REGULUS-50-I2 fed with iodine propellant developed at Technology for Propulsion and Innovation (T4i).

REGULUS-50-I2 technology relies on the MEPT which is integrated into a complete propulsion unit of 1.5 U, with a total mass which is below 3 kg in the 3 kNs version. An expanded version of the propulsion system with a total impulse of about 7 kNs shal be developed for the e.Inspector mission.

Several improvements are introduced to take into consideration the mission requirements:

- a re-designed fluidics sub-system, with optimized thermal design
- a bigger tank, to accommodate enough iodine for 7 kNs
- an improved thermal control of electronic boards, contained in the thruster sub-system
- a higher maximum heating power, brought from 20 W to 40 W.
- CAN-bus communication interface, more robust with respect to the initial I2C

The preliminary features of this new REGULUS-50-I2 7 kNs system are summarized in Table 5.2-4, as well as its layout.

*Table 5.2-4. REGULUS-50-I2 features.*

| Feature | Value |
|---|---|
| Thrust | 0.25 – 0.65 mN (0.55 mN @50 W) |
| Specific Impulse | Up to 650 s (550 s @ 50 W) |
| Input Power | 30 – 60 W (60 W nominal) |
| Mass Flow | 0.1 mg/s |
| Propellant | Iodine ($I_2$) |
| Volume | 93.0 mm x 95.0 mm x 200.0 mm (2 U) @ 7000 Ns |
| Weight | 4 kg @ 7000 Ns (wet mass) |
| Electric Interface | 12 V DC regulated |
| Communications | Can-bus or I2C with CSP protocol |

*CAD of REGULUS-50-I2 7kNs.*

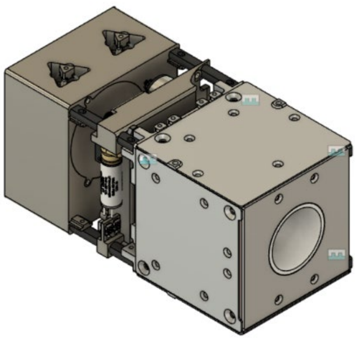

The selected backup option as primary propulsion unit is the ENPULSION NANO R$^3$ thruster with Gamma (γ) emitters, in order to ensure the level of performance that is required by the e.Inspector mission. This option provides a more compact alternative that fits in one CubeSat unit and consumes around 45 W at maximum, while also providing great flexibility by allowing to operate the thruster along the full dynamic range throughout the mission. The largest disadvantage is the low thrust level that must be traded-off with the total impulse that can be provided by the unit. Assuming to desire the same total impulse of the baseline unit, about half the thrust would be available, resulting in double transfer times.

*Table 5.2-5. ENPULSION NANO R3 features.*

| Feature | Value |
|---|---:|
| Thrust | 0.10 – 0.35 mN (0.35 mN @45 W) |
| Specific Impulse | 1000 - 5000 s (2000 @ 45 W) |
| Total Impulse | More than 400 Ns |
| Input Power | 20 – 45 W (45 W nominal) |
| Volume | 98.0 mm x 99.0 mm x 95.3 mm (1 U) |
| Weight | 1.4 kg (wet mass) |
| Electric Interface | 12 V/ 28 V DC regulated |

| | |
|---|---|
| Communications | RS422/RS485 |

### 5.2.2-1 Secondary Propulsive Unit

The secondary propulsive unit is responsible for providing thrusting capabilities during the relative manoeuvring phase. As such, higher thrust capabilities and the possibility to quickly switch on/off the thruster are main driving characteristics. In this context, chemical solutions performs better than the electric solution considered for the primary propulsion.
A trade-off analysis was performed on two different chemical propulsive solutions: the Vacco Propulsion Unit for Cubesat (PUC) and the IANUS thruster by T4i. Table 5.2-6 below reports the main features and metrics of both.

*Table 5.2-6: Comparison of secondary propulsive units main metrics; VACCO propulsion unit*

| Feature | VACCO | IANUS |
|---|---|---|
| Thrust | Up to 5.5 mN | 6.8 to 26.2 mN |
| Power | Up to 18 W | 40 W |
| Total Impulse | Up to 123 Ns | 38 Ns |
| Wet Mass | 589 g | 500 g + propellant |
| Envelope | 0.14 U + Tuna Can | 0.5 U |
| Country | USA | ITA |
| TRL | 8 | 8 |
| Propellant | High Purity Liquid Sulfur Dioxide | R134a |

The propulsion unit from Vacco has higher thrust values and it can also be placed in the Tuna Can volume of the deployer, thus leaving more free envelope in the 12U structure. The IANUS thruster is a European product, and it is produced by T4i, that is the provider of the primary propulsion unit. Despite the higher thrust of the IANUS, the higher total impulse makes the VACCO PUC a more robust alternative. In addition, the fact that it can be inserted in the tuna can is fundamental to achieve a feasible configuration that satisfies all system-related constraints while maintaining a symmetric thrust centre. Thus, the selected baseline is to have two units of the Vacco Propulsive Unit for CubeSat (PUC), in order to be used at the same time to avoid angular momentum accumulation. The two units together satisfy the total impulse requirement, correspondent to a value larger than 79 Ns. IANUS system by T4i is kept as bakup.

### 5.2.3 Structure and Configuration design

Phase A closed in favor of a 12U standard COTS CubeSat structure.
The configuration is the more affected by the 2U EPU,the VACCO PUC 2 elements and the microsada accommodation. The COTS 12U structure from 2nd-Space allows selecting a central-slotted frame designed to allow the EPU to be mounted in correspondence of the symmetry axis of the structure itself, resulting in the optimal choice for the e.Inspector mission.
Additionally, the VIS and TIR payloads, as well as the start tracker, has been located in order to avoid any occlusion and to limit as much as possible the presence of the Sun and/or the Earth in the FOV. An overview of the baseline configuration is reported in Figure 5.2-5.
The deployable and orientable solar arrays are showed in deployed configuration. Additional cells are placed in the body mounted panels on the top side (+z) and on the face with the openings for the payloads (-y) to handle the non-nominal cases. It is acknowledged that the SADA mechanism reported in the figure is a simplified version. Iterations with the provider are ongoing to define the final envelope, in particular of

the mechanism rectangular box, with the objective to avoid any deviation from standard 12U PODs. Both the VIS and TIR cameras are pointing in the same direction on the same face in order to ensure the observability of the target with both the cameras avoiding any occlusion, also from the movable deployable solar arrays (notice that the payloads are located on the face opposite to the SADA, avoiding that the deployable solar arrays enter the payloads FOV for all the rotation angles). On the same face are located the High Gain S antenna and the Low Gain S antenna. A GPS antenna is located on the face opposite to the cameras in order to maximize the visibility. On the same side is located also the second Low Gain S antenna. As already mentioned, the CGs are located on the top panel (protruding from it), as well as the other GPS antenna to maximize the visibility.

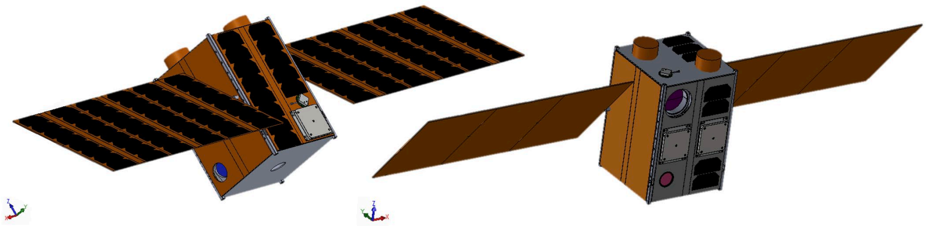

*Figure 5.2-5: e.Inspector baseline outer configuration*

The inner configuration is showed in Figure 5.2-6 with reference to the main components. The stack components (TT&C, OBDH, and EPS stack components) are located in the same 1U bay in order to minimize the harness complexity. The same holds for the RWs assembly, the magnetorquer and the IMUs. The envelope allocated for the TIR camera is about 1.5U in order to have enough free volume back to the TIR to accommodate the GNC boards (i.e., the DOCK-CAM and the IF-BOARD-GNC) and the DOCK-ADCS. In Figure 5.2-6 it can be noticed that the EPU is located in the central axis of the 12U structure and mounted on a frame with a central slot. The configuration discussed here allows to fulfil the requirements about the CoM position with respect to the thrusting axis, resulting to be about 12.15mm, below the maximum admissible value of 2cm. Further, notice that the SADA mechanism is located inside the envelope of the 12U structure, avoiding lateral protrusion and ensuring the compatibility with deployers as the ExoPod NOVA (TRL9 since 2022).

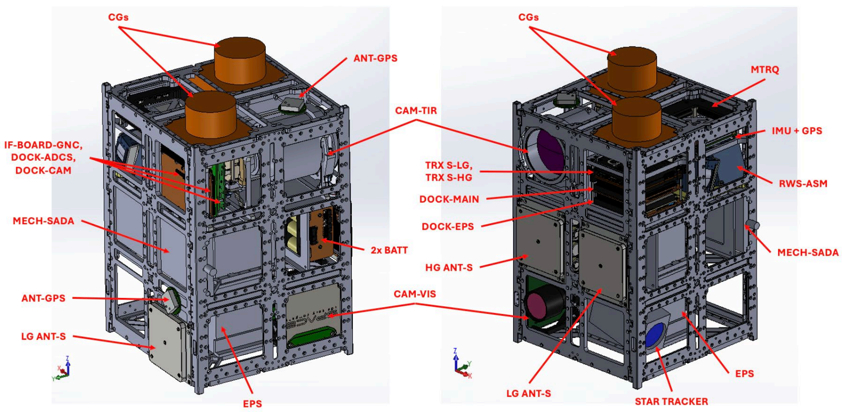


*Figure 5.2-6: e.Inspector baseline inner configuration*

### 5.2.4 Telemetry, Tracking & Telecommand Subsystem Design

The baseline at the end of phase A considered as payload channel an S-band link, and as low capacity channel the VHF band. Phase B showed the benefit in considering S-band link for the low capacity channel as well. Changes are synthetized in Table 5.2-5.

*Table 5.2-7: comparison of Phase A baseline and phase B baseline.*

| | Previous baseline | New Baseline |
|---|---|---|
| **Low capacity channel** | VHF<br>Skylabs NANOcomm<br>ISISpace deployable VHF antenna | S-Band<br>GOMSpace NanoCom AX2150<br>GOMSpace NanoCom AM2150-P/PS couple of patch antennas. |
| **High capacity channel** | S-Band<br>Skylabs NANOlink<br>2x Skylabs patch antennas (RX + TX) | S-Band<br>GOMSpace NanoCom SR2000<br>GOMSpace NanoCom ANTS2000<br>(2x, cold redundancy) |

The telemetry and telecommand links are supported by a low gain S-band channel (SLG), while for the payload data transmission, a high gain S-band channel (SHG) is considered as baseline.
A relevant part of the channel design is the compliance with ITU power flux density (PFD) limitations, which provide an upper boundary in the downlink, during any possible worst case scenario. In particular for the S-Band, this value is equal to -144 dB/m$^2$/4kHz for 90° elevation angles. Such imposition, constraints very much the channel capacity, in particular for safe modes, where the gain value of the antenna to be considered for link budget analyses is far lower than the maximum one to be used for PFD computations. Moreover for the eInspector mission, the link budget worst case distance is given by the 790 km altitude orbit of the baseline target with 5° elevation, while the PFD worst case is given by the secondary targets at 550km altitude at 90° elevation. As a consequence, a proper tuning of RF output power and bandwidth is needed. The downlink design is done in accordance to the worst case scenario, where the highest data volume of 14.07 GB (20% margined) has to be downlinked just after one inspection phase.
Table 5.2-6 lists the expected data budget for each inspection phase: number of images is computed considering one image (both VIS and IR) each 20 minutes when the distance is over 1600m, and 2 minutes when the distance is under the threshold.

*Table 5.2-8 Inspection phases data budget.*

| Inspection ID | Imaging Time [h] | Data Volume [GB] | #images | GS contacts | Downlink Time [min] |
|---|---|---|---|---|---|
| IO#1 | 24 | 2.02 | 280 | 48 | 447 |
| IO#2 | 12 | 2.52 | 350 | 59 | 559 |
| IO#3 | 12 | 4.16 | 578 | 98 | 923 |
| IO#4 | 36 | 14.07 | 1954 | 329 | 3119 |

Table 5.2-7 reports the link budgets for the SHG channel both in Up- and Downlink.

*Table 5.2-9: Link Budgets for the SHG link in the nominal scenario*

| | SHG Uplink | SHG Downlink |
|---|---|---|
| Frequency [MHz] | 2080.00 | 2260.00 |
| Bandwidth [kHz] | 2000.00 | 1800.00 |
| Net datarate [kbps] | 897.36 | 807.62 |
| Gross datarate [kbps] | 3333.33 | 3000.00 |
| Symbolrate [ksps] | 1666.67 | 1500.00 |
| RF out power [W] | 25.00 | 1.58 |
| RF out power [dBW] | 13.98 | 2.00 |
| RF out power [dBm] | 43.98 | 30.00 |

| | | |
|---|---|---|
| Gain TX [dBi] | 34.60 | 8.00 |
| Loss TX line [dB] | -0.50 | -0.50 |
| Loss misalign. point + polarisation [dB] | -1.50 | -1.50 |
| EIRP [dB] | 48.08 | 7.50 |
| Loss Free Space [dB] | -167.63 | -168.35 |
| Loss ATM + IONO [dB] | -3.85 | -3.85 |
| Loss RX line [dB] | -0.50 | -0.50 |
| Gain RX [dBi] | 8.00 | 34.60 |
| RX Noise Figure [dB] | 6.19 | 1.86 |
| T noise RX [K] | 917.06 | 155.00 |
| G/T [dB/K] | -21.62 | 12.70 |
| EbN0 required [dB] | 6.00 | 6.00 |
| SNR real [dB] | 18.56 | 12.04 |
| SNR target [dB] | 9.01 | 9.01 |
| **Data Link Margin [dB]** | **9.55** | **3.03** |

SLG occur through patch antennas. This approach has been preferred over a deployable omnidirectional antenna, due to the higher gain pattern performance expected by datasheet.
The SLG transceiver is kept always switched on in all the operative modes to ensure the availability of a communication channel allowing the spacecraft to receive telecommands at any time during the mission.Table 5.2-8 shows the link budget for the SLG link.

*Table 5.2-10: Link Budgets for the SLG link in the nominal scenario*

| | SLG Uplink | SLG Downlink |
|---|---|---|
| Frequency [MHz] | 2080.00 | 2260.00 |
| Bandwidth [kHz] | 137.00 | 114.17 |
| Net datarate [kbps] | 59.22 | 49.35 |
| Gross datarate [kbps] | 96.00 | 80.00 |
| Symbolrate [ksps] | 96.00 | 80.00 |
| RF out power [W] | 25.00 | 0.10 |
| RF out power [dBW] | 13.98 | -10.00 |
| RF out power [dBm] | 43.98 | 20.00 |
| Gain TX [dBi] | 34.60 | 5.50 |
| Loss TX line [dB] | -0.50 | -0.50 |
| Loss misalign. point + polarisation [dB] | -1.50 | -1.50 |
| EIRP [dB] | 48.08 | -5.00 |
| Loss Free Space [dB] | -167.63 | -168.35 |
| Loss ATM + IONO [dB] | -3.85 | -3.85 |
| Loss RX line [dB] | -0.50 | -0.50 |
| Gain RX [dBi] | 5.50 | 34.60 |
| RX Noise Figure [dB] | 4.44 | 1.86 |
| T noise RX [K] | 515.70 | 155.00 |
| G/T [dB/K] | -21.62 | 12.69 |
| EbN0 required [dB] | 7.00 | 7.00 |
| SNR real [dB] | 30.20 | 11.52 |
| SNR target [dB] | 7.00 | 7.00 |
| **Data Link Margin [dB]** | **23.20** | **4.52** |

### 5.2.5 Electric Power Subsystem Design

The main trade-off performed on the EPS sub-system during the Phase B concerned the Solar Panels

mounting strategy. This trade-off belongs to the high-power request by the Electric Propulsive Unit, which shall be guaranteed during the transfer phase. A solution with SADA turned out to be adequate (see Figure 5.2-5). This configuration consists of a couple of triple-folded wings equipped with 18 cells per folding, for a total number of cells mounted on the wings equal to 108. The wings with a SADA mechanism add a further degree of freedom in addition to the roll angle, enlarging the chance to optimize the incoming energy.
The overall peak power in sun pointing mode is Pmax = 121 W. [RD poer moede] reports all modes and phases energy budgets needed and supplied. The selected cells are the CTJ30 SDA with a 27.5 cm^2 form factor. The baseline SADA system selected is the µSADA system from IMT Technology due to the complete compatibility with the solar panels and the EPS system. The backup solution is the microSADA system from DHV, that shows similar performances, but needs to be customised to be mounted inside the volume of the 12U.
e.Inspector is equipped with a battery pack which complies with 10700 cycles. The necessary BoL capacity is 140 Wh, which ensures the electric thruster utilisation available in eclipse also. For those reasons, two GOM Nanopower BPX, total capacity is 154 Wh and configuration 4s2p is selected. The supplier also gives the possibility to have an 8s configuration. The 4s2p baseline is selected to have redundant string in case of failure in a cell. ClydSpace and ISISpace solutions are kept as backups.
ACU and the PDU mounted on a single EPS board for power control is adopted, being available as COTS. The GomSpace products are comparable to ISISpace products in terms of performance and system redundancies but are considered here more reliable because of the longer flight heritage. Moreover, the PoliMi team has a quite strong direct expertise with the GOMSpace EPS system. For this reason, GOMSpace components are selected as baseline, while ISIS is kept as backup.
To manage the relatively high power coming from the Solar Panels and to correctly distribute the power to the other subsystems the EPS components configuration includes 2 PDU and 2 ACU.
An aspect of the EPS subsystems that will require further investigation in the next design phases is the transient response of the thruster during startup, as the high energy demand might pose criticalities in bus stability. Also, if a thrusting arc is continued during a sunlight to eclipse transition the increased load on the battery might be problematic to the voltage regulation of the system. As proposed by the main propulsion system supplier, further considerations are postponed to the next phases, as it is necessary to test the propulsion unit on a representative bus model.

### 5.2.6 On-board Data Handling design

A detailed description of the OBDH subsystem proposed for the study is reported in [AD5].
A strong requirement in the selection of the OBC motherboard architecture is that each service module component shall have flight heritage at the date of launch. Given the complexities of the algorithms compared to the size of the mission, it is necessary to carefully plan and develop the maturity level of the subsystem also in terms of hardware, comprising, as mentioned, only components with flight heritage.
The required architecture features four main components: OBC-MAIN, OBC-GNC, DOCK-GNC and OBC-CAM. The GNC and OBDH systems entail several required functionalities here grouped.

*Table 5.2-11: Functionalities of OBDH-GNC computing system.*

| Component | COTS | Description |
|---|---|---|
| **OBC-GNC** | Yes | OBC in charge for acquisition of sensor readings, control actuation, part of GNC algorithms (TBC). |
| **DOCK-GNC** | Yes | Routing board feeding signals generated by OBC-GNC to sensors and actuators. |
| **OBC-MAIN** | Yes | OBC in charge of monitoring S/C health status, collecting telemetry, running central software, interfacing with radios. |

| | | |
|---|---|---|
| **OBC-CAM** | Yes | OBC in charge of execution of image processing and vision-based navigation algorithms, together with some computationally demanding GNC modules strongly linked to the IP output. |

Three different architectures have been traded off according to:

- Electrical interfaces availability
- Data protocol interfaces
- Programming flexibility (driver coding, algorithms deployment, etc.)
- Computational power
- COTS (in general, need for customization: the higher the less customization or custom components are needed)
- Cost
- Lead time

Table 5.2-10 details the baseline architecture selected, while Figure 5.2-3 shows the overall schematics.

*Table 5.2-12: baseline architecture OBC-CAM: high performance CPU featuring an FPGA core, OBC-MAIN and OBC-GNC baseline.*

| Component | Flight Heritage | Product |
|---|---|---|
| OBC-GNC | Yes | GomSpace A3200 |
| DOCK-GNC | Yes | GomSpace ADCS6 |
| OBC-MAIN | Yes | GomSpace A3200 |
| DOCK-MAIN | Yes | GomSpace DMC3 |
| OBC-CAM | Yes | Xiphos Q8 |
| CAM-BOARD | Yes | Q8 Camera Board |
| OBC-PIM | Yes | Q8 PIM |

In addition to the mentioned components, a custom interface board is required, in order to provide enough peripherals to connect all the AOCS components to the GNC-OBC. For budgeting purposes, the mass and volume of a single GOMSpace ADCS-6 docking board are taken in consideration. The rerouting and data protocol conversion features that this IF-BOARD-GNC needs to provide are the following:

- UART to RS485 conversion, to interface the Star Tracker to the OBC
- CAN to 2x RS422 conversion, to interface to the two cold gas thrusters
- Power lines to feed the two cold gas thrusters
- Power and data switch to control the two IMUs used in cold redundancy and connected to the CAN bus
- Power and data to control the secondary GNSS receivers used in cold redundancy and connected to the UART line

Moreover, for connection easiness, the IF-BOARD-GNC shall have a stack PC104 connector, in order to receive power lines for the thrusters.

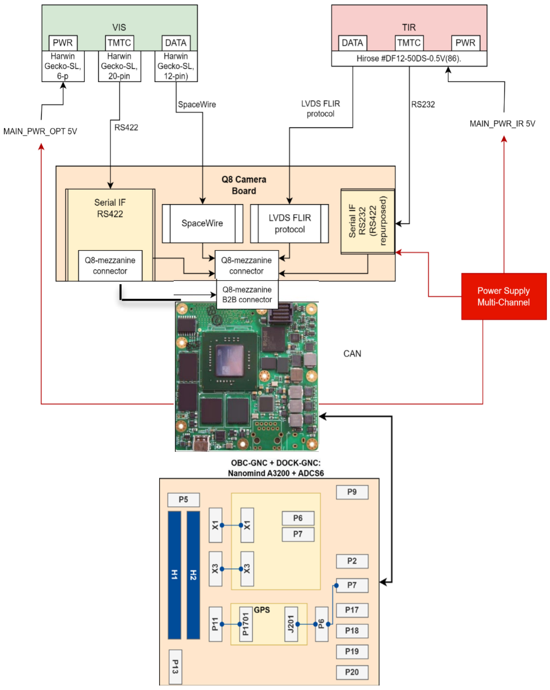


*Figure 5.2-7: Detailed OBDH architecture*

# 6 System budgets

Figure 6-1 represents the product tree of the space segment, by subsystem. Light-grey elements represent virtual components, i.e. those elements included already within other items, reported for clarity.


*Figure 6-1: Product tree of the space segment.*

The total system mass with subsystem level margins only amounts to 19.4 kg, as broke down in Table 6-1. Adding a 10% system level margin, the total mass reaches 21.4 kg. The presented mass budget is already including secondary structures, harness and fasteners in the global estimation. The considered deployer by Exolaunch (EXOpod Nova) provide a maximum launchable mass of 32kg. As a consequence, with the current baseline design, there is a total mass margin of around 10 kg.

*Table 6-1: Mass Budget.*

| Name | Description | Mass [g] | M% | M.Mass [g] |
|---|---|---|---|---|
| **PFM/FM0 (with system margin)** | | | | **21384.2** |
| **System margin** | | | **10%** | |
| **PFM/FM0** | **Spacecraft** | **17449.1** | | **19440.1** |
| **PAYLOAD** | **Payload** | **864.9** | | **951.4** |
| CAM-VIS | Visible camera | 390.0 | 10% | 429.0 |
| CAM-IR | Far infrared camera | 474.9 | 10% | 522.4 |
| **TCS** | **Thermal Control System** | **344.0** | | **378.4** |
| TS-EPU4 | Regulus aluminum thermal strap | 81.0 | 10% | 89.1 |
| HTR-STR | Star tracker heater | 20.0 | 10% | 22.0 |
| TS-EPU1 | Regulus aluminum thermal strap | 81.0 | 10% | 89.1 |
| TS-EPU3 | Regulus aluminum thermal strap | 81.0 | 10% | 89.1 |
| TS-EPU2 | Regulus aluminum thermal strap | 81.0 | 10% | 89.1 |
| **OBDH** | **On-Board Data Handling** | **217.0** | | **240.6** |
| DOCK-CAM | Camera Board | 56.0 | 20% | 67.2 |
| OBC-MAIN | On-board computer | 24.0 | 5% | 25.2 |
| DOCK-MAIN | Docking board hosting MAIN-OBC and SLG TRX | 51.0 | 5% | 53.6 |
| OBC-CAM | On-board computer | 56.0 | 10% | 61.6 |
| PIM-CAM | | 30.0 | 10% | 33.0 |
| **EPS** | **Electric Power System** | **4018.0** | | **4602.7** |
| ACU-2 | Array Conditioning Unit | 54.0 | 5% | 56.7 |
| SADA | sada | 236.0 | 10% | 259.6 |
| PDU-1 | Power Distribution Unit 1 | 57.0 | 5% | 59.9 |
| BATT-1 | Battery pack number 1 | 500.0 | 5% | 525.0 |
| ACU-1 | Array Conditioning Unit | 54.0 | 5% | 56.7 |
| B-SArray-ASM | Body-mounted Solar Array Asm | 400.0 | 20% | 480.0 |
| W-SArray-ASM | Wing Solar Array Asm | 2080.0 | 20% | 2496.0 |
| DOCK-EPS | EPS docking board | 80.0 | 5% | 84.0 |
| BATT-2 | Battery pack number 2 | 500.0 | 5% | 525.0 |
| PDU-2 | Power Distribution Unit 2 | 57.0 | 5% | 59.9 |
| **TTMTC** | **Telemetry, Telecommands, and Control** | **599.0** | | **657.3** |
| ANT-SLG-1 | S-band LG antenna patch 1 | 93.0 | 10% | 102.3 |
| TRX-SHG | S-band HG transceiver | 271.0 | 10% | 298.1 |
| TRX-SLG | S-band LG transceiver | 32.0 | 5% | 33.6 |
| ANT-SHG | S-band HG antenna | 110.0 | 10% | 121.0 |
| ANT-SLG-2 | S-band LG antenna patch 2 | 93.0 | 10% | 102.3 |
| **GNC** | **GNC Subsystem** | **2454.4** | | **2586.7** |
| FSS+X2 | Fine Sun Sensor +X2 | 2.2 | 5% | 2.3 |
| GNSS-1 | GNSS receiver | 31.0 | 5% | 32.6 |
| FSS+Z2 | Fine Sun Sensor +Z2 | 2.2 | 5% | 2.3 |
| OBC-GNC | GNC Controller | 24.0 | 5% | 25.2 |
| FSS+Z1 | Fine Sun Sensor +Z1 | 2.2 | 5% | 2.3 |
| MTORQ | 3-axis Magnetorquers | 156.0 | 5% | 163.8 |
| FSS+Y1 | Fine Sun Sensor +Y1 | 2.2 | 5% | 2.3 |
| FSS-X2 | Fine Sun Sensor -X2 | 2.2 | 5% | 2.3 |
| GNSS-ANT-1 | GNSS antenna | 50.0 | 5% | 52.5 |
| DOCK-GNC | GNC Docking Board | 64.0 | 5% | 67.2 |
| IMU-2 | Inertial Measurement Unit | 90.0 | 5% | 94.5 |
| FSS-Y2 | Fine Sun Sensor -Y2 | 2.2 | 5% | 2.3 |
| GNSS-2 | GNSS receiver | 31.0 | 5% | 32.6 |
| ST | Star Tracker | 270.0 | 5% | 283.5 |
| FSS+X1 | Fine Sun Sensor +X1 | 2.2 | 5% | 2.3 |
| MAGMTR | Main Magnetometer | 8.0 | 5% | 8.4 |
| FSS-Y1 | Fine Sun Sensor -Y1 | 2.2 | 5% | 2.3 |
| FSS-Z1 | Fine Sun Sensor -Z1 | 2.2 | 5% | 2.3 |
| FSS-Z2 | Fine Sun Sensor -Z2 | 2.2 | 5% | 2.3 |
| IF-BOARD-GNC | GNC interface Board | 64.0 | 20% | 76.8 |
| FSS-X1 | Fine Sun Sensor -X1 | 2.2 | 5% | 2.3 |
| GNSS-ANT-2 | GNSS antenna | 50.0 | 5% | 52.5 |
| FSS+Y2 | Fine Sun Sensor +Y2 | 2.2 | 5% | 2.3 |
| IMU-1 | Inertial Measurement Unit | 90.0 | 5% | 94.5 |
| RWL-ASM | Reaction wheel assembly | 1500.0 | 5% | 1575.0 |
| **HARNESS** | **Platform harness** | **400.0** | **20%** | **480.0** |
| **STR** | **Structure and Mechanisms** | **3373.8** | | **4047.3** |
| RW-ASM-MECH | RWS mechanical support | 250.0 | 20% | 300.0 |
| GNS-STANDOFF-2 | | 3.1 | 0% | 3.1 |
| GNSIMU-MECH | GNSS-IMU mechanical support | 64.0 | 20% | 76.8 |
| STR-PRM | Primary Structure | 2740.0 | 20% | 3288.0 |
| GNS-STANDOFF-1 | | 3.1 | 0% | 3.1 |
| VISCAM-MECH | VIS camera mechanical support | 80.0 | 20% | 96.0 |
| IRCAM-MECH | NIR camera mechanical support | 233.6 | 20% | 280.3 |
| **SOFTWARE** | **On-board Software** | **0.0** | | **0.0** |
| **PROP** | **Propulsion** | **5178.0** | | **5495.8** |
| THRUSTER-CG-1 | Cold Gas thrusters - PUC | 589.0 | 10% | 647.9 |
| THRUSTER-CG-2 | Cold Gas thrusters - PUC | 589.0 | 10% | 647.9 |
| THRUSTER-ASM | Thruster assembly ($w_/$ propellant) | 4000.0 | 5% | 4200.0 |

*Table 1 – concluded*

Table 6-2 reports the power consumption per each subsystem and for all the relevant mission modes. A total margin of 20% is then considered at system level. The most demanding mode is represented by the TRANS mode, where the electric propulsion system is active, reaching a maximum of 81 W, representing the sizing condition for the solar arrays.

*Table 6-2: Power budget for the most relevant mission modes.*

| **Power Consumption [W]** | MODE | | | | |
|---|---|---|---|---|---|
| | **LEOP** | **TRANS** | **REL-MAN** | **COM-HG** | **SAFE** |
| **PL** | 0.000 | 0.000 | 4.620 | 0.000 | 0.000 |
| **GOC** | 2.955 | 8.884 | 10.288 | 10.288 | 5.830 |
| **EPS** | 0.870 | 1.920 | 1.920 | 0.870 | 0.975 |
| **OBDH** | 0.293 | 0.293 | 3.335 | 0.585 | 0.585 |
| **PROP** | 0.000 | 56.100 | 1.760 | 0.000 | 0.000 |
| **TTMTC** | 0.189 | 0.189 | 0.189 | 18.239 | 1.890 |
| **STR** | 0.000 | 0.000 | 0.000 | 0.000 | 0.000 |
| **TCS** | 1.980 | 0.198 | 0.000 | 0.000 | 0.198 |
| **System** | 6.287 | 67.584 | 22.113 | 29.982 | 9.479 |
| **System w/ 20% margin** | 7.545 | 81.101 | 26.535 | 35.979 | 11.375 |
| **Average power production for baseline target debris (39162)** | 10.724 (folded, tumbling) | 82.729 | 68.476 (holding point), 78.622 (inspection orbit) | Depending on eclipse cycle and ground station | 89.455 (Sun pointing) |

Table 6-3 sums up the technology readiness (TRL) level of all the components of the eInspector platform.

*Table 6-3: Components TRL recap*

| Name | Component | Provider | TRL | Source |
|---|---|---|---|---|
| **PAYLOAD** | | | | |
| CAM-VIS | GECKO Imager | Dragonfly Aerospace | 9 | nSight-1, LiciaCube, CUMULOS |
| CAM-IR | FLIR TAU 2 | FLIR | 9 | Phoenix Cubesat |
| **OBDH** | | | | |
| OBC-MAIN | NanoMind A3200 | GOMSpace | 9 | GOMX-flight program |
| OBC-CAM | Xiphos Q8 | Xiphos | 9 | GHGSat - C Series |
| DOCK-MAIN | DMC3 | GOMSpace | 9 | GOMX-flight program |
| DOCK-CAM | Q8 Camera Board | Xiphos | 9 | GHGSat - C Series |
| PIM-CAM | Q8 PIM | Xiphos | 9 | GHGSat - C Series |
| **EPS** | | | | |
| ACU | ACU-200 | GOMSpace | 9 | GOMX-flight program |
| PDU | PDU-200 | GOMSpace | 9 | GOMX-flight program |
| BATT | NanoPower BPX | GOMSpace | 9 | GOMX-flight program |
| DOCK-EPS | P60Dock | GOMSpace | 9 | GOMX-flight program |
| SADA | $\mu$SADA | IMT Technology | 6 | TTRL8 Q1/2 2025 as per IMT test plan |
| Solar Array | 18-cell panel | IMT Technology | 6 | TTRL8 Q1/2 2025 as per IMT test plan |
| **TMTC** | | | | |
| TRX-SHG | NanoCom SR2000 | GOMSpace | 9 | GOMX-flight program |
| TRX-SLG | NanoCom AX2150 | GOMSpace | 9 | GOMX-flight program |
| ANT-HSG | NanoCom ANT2000 | GOMSpace | 9 | GOMX-flight program |
| ANT-HLG | NanoCom AM2150-P/PS | GOMSpace | 9 | GOMX-flight program |
| **GNC** | | | | |
| OBC-GNC | NanoMind A3200 | GOMSpace | 9 | GOMX-flight program |
| DOCK-GNC | NanoDock ADCS6 | GOMSpace | 9 | GOMX-flight program |
| GNSS | Novatel OEM719 | Novatel Inc. | 9 | Pumpkin |
| FSS | NanoSense FSS | GOMSpace | 9 | GOMX-flight program |
| IMU | MS-IMU3050M | Memsense Inc. | 9 | |
| MAGMTR | RM3100 | PNI Sensor Corp. | 9 | GOMX-flight program |
| MTROQ | GST-600 | GOMSpace | 9 | GOMX-flight program |
| RWL | RW400 | Hyperion Tech. | 9 | Claimed by AAC Clyde Space |
| ST-ASM | Sagitta ST | Arcsec | 9 | ESA IOD CubeSats |
| IF-BOARD-GNC | - | - | 4 | Custom design |
| **PROP** | | | | |
| THRUSTER-CG | VACCO PUC | VACCO/CU Aerospace | 6 | CU Aerospace datasheet |
| THRUSTER-ASM | REGULUS-50-I2 | T4i | 7 | - |
| **STR** | | | | |
| STR-PRM | Verse-12 (Custom) | 2NDSpace | 6 | TTRL8 at procurement |
| All MECH | SADA HDRM | IMT | 6 | TTRL8 Q1/2 2025 as per IMT test plan |

# 7 Ground Segment Design

The Ground Segment is composed of the following three components:

- Ground Station Network (GSN)
- Mission Operation Centre (MOC)
- Distribution or Mission Data delivery

The two first alternatives have been traded off according to cost, reliability, security, flexibility. Dedicated GSN against a ground as a service solution were compared selecting the latter, provided by Leaf Space srl: GSaaS solution allows leveraging on already existing ground segment services designed to be highly reliable and to satisfy different mission requirements. Typically, the use of these services has a consumption-based cost allowing to reduce the CAPEX and the overall cost thanks to leveraging on already available and operational Ground Station Network and Mission Control Software/Service. Flexibility is generally a peculiar characteristic of these services since they support different missions with different requirements and a change can be addressed with a limited impact on cost and planning. Thanks to the need to support several missions coming from different owners (commercial companies, space agencies, government agencies) high security levels and procedures are strictly adopted and updated.
A physical versus a virtual solution were compared as far as the MOC is concerned, selecting the latter; that allows to leverage on the flexibility provided by server-client Mission Control Software architectures where it is only needed to have the server running in a safe and reliable environment with multiple clients connected to it used as interfaces by the mission operators. This architecture could be even more simplified by having the MCS server running in a cloud environment and leveraging on the native reliability and security of such technology, with access to it provided through the clients that can typically run on any internet browser with dedicated credentials. Moreover, the adoption of virtualized MOC solution allows a fast implementation and reduced startup time in order to have a fully running reliable, secure and cost-effective system.
The last line of trade-off, MCS, drove to the LeanSpace MCS being modular, flexible and ready to be interfaced with the LeafSPace GS.
eInspector is expected to ask for 5-10 contacts per day during LEOP, 3 contact per day to manage telemetry and telecommand. The payload download is expected to ask for 18Gb/day volume to manage.
The Leaf Space array, with 26 antennas considered, can easily offer a minimum of 40 passages/day for a 365 min daily contacts 300s each ad minimum. The Leaf Line services, provided by the Ground Stations Network, enable customers to operate their spacecrafts for TT&C in S-Band and for payload data downlink. The schema in Figure 7-1 is detailing how the Leaf Line services are handling data for both TT&C and payload downlink, implemented in S-Band, including the interfaces with the Space Segment, on one side, and the Mission Control Software, on the other.

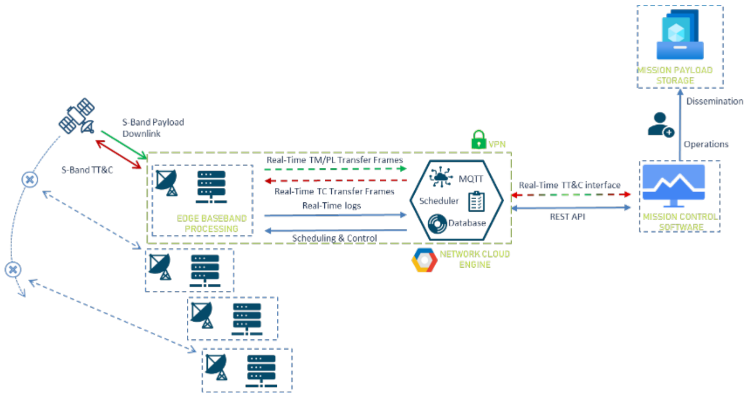


*Figure 7-1 - S-Band data flow and Interfaces*

# 8 Final remarks

The phase B allowed consolidating the IP-GNC HW architecture and developing the core of the iP-GNC SW from the IP to the navigation, guidance and control.
The PIL and HIL campaigns for the IP confirmed the validity of the designed architectures both for the SW and the HW.
The subsystem design showed the mission feasibility with COTS or slightly customized TRL8/9 components.
The already detected critical item in the electric PS is confirmed and the still to be finalized endurance test campaign shall be kept going up to the endo of the next phase C.
The proposed COTS payloads are confirmed with the need to keep going testing and characterizing the IR camera to calibrate the synthetic images generator for the IR images datasets.
The more rigid re-entry regulations affect the mission feasibility imposing as target a lower debris to be completely robust to any potential failure at the launcher release as well. However the mission keeps feasible even with a possible change on target.

End of document